Ultraviolet to infrared downshifting in Ce and Yb co-doped aluminum oxynitride thin films

Alaa E Giba, P Pigeat, S Bruyere, Hervé Rinnert, F Soldera, F Mücklich, R Gago, David Horwat

Ultraviolet to Infrared downshifting in Ce and Yb co-doped Aluminum oxynitride thin films

Alaa E. Giba[1,2,3*], P. Pigeat[1], S. Bruyere[1], H. Rinnert[1], F. Soldera[2], F. Mücklich[2], R.Gago[4], D. Horwat[1]

[1]*Institut Jean Lamour – UMR CNRS 7198– Université de Lorraine, Nancy, France.*

[2]*Department Materials Science and Engineering, Saarland University, D-66123 Saarbrücken, Germany.*

[3]*National Institute of Laser Enhanced Sciences, Cairo University, Giza 12613, Egypt*

[4]*Instituto de Ciencia de Materiales de Madrid, Consejo Superior de Investigaciones Científicas, E-28049 Madrid, Spain.*

* contact : alaa-eldin-abdel-azi.giba@univ-lorraine.fr

Abstract

We report for the first time on ultraviolet (UV) to near infrared (NIR) downshifting (DS) between cerium, Ce, and Ytterbium, Yb, in aluminum oxynitride, Al(O)N, thin films prepared by reactive magnetron sputtering technique. The crystal structure of the prepared samples has been investigated by X-ray diffraction (XRD) and transmission electron microscopy (TEM). In addition, the content of Ce and Yb were determined by Rutherford backscattering spectrometry (RBS). The role of Ce in downshifting the absorbed excitation UV photons into NIR ones is supported by photoluminescence (PL) and photoluminescence excitation (PLE) measurements of (Ce, Yb) co-doped samples. Time-resolved PL (TRPL) along with PL power-dependent measurements propose that *one-to-one* photon mechanism is achieved through charge transfer state (CTS) mediation. The present findings contribute to the racetrack of downconversion (DC) solar cell topic by investigating such DC phenomenon in a new matrix, Al(O)N.

Keywords: Downshifting, Ce to Yb charge transfer, Aluminum oxynitride.

1. Introduction

Downconversion silicon solar cell attracts considerable interest due to its potential in improving the solar cell efficiency. The mismatch between the sunlight spectrum and the spectral response of Si, except narrow range in near infrared, limits the cell efficiency owing to the loss of a significant part of the UV-Visible region of the solar spectrum via thermal

dissipation. Hence, extensive efforts have been devoted to down-convert UV-visible photons into IR radiation. For this purpose, luminescent materials doped with rare earth ions have been recently investigated[1-5]. Ytterbium (III), coupled with other ions, is the most promising ion used in this direction. $Yb^{3+}$is the last RE^{3+} ion exhibiting incomplete 4*f* orbital. Yb^{3+}exhibits simple electronic configuration, $F_{7/2}$ and $F_{5/2}$, thanks to the spin-orbit interaction. In addition the emission spectrum of Yb^{3+} fall in the near infrared region (NIR) around 1000 nm, which is fully matching with the maximum of spectral response of Silicon[6-8]. Therefore, researches are directed to find a way to transfer UV-VIS photons of the solar radiation into NIR by downconversion or downshifting of the energy from mediator ion(s) to the Yb. Then the excited Yb ions further transfer the energy to silicon which is supposed to enhance functionalized solar cells efficiency. This approach can be realized via energy transfer of one UV-Visible photon to either one (downshifting, DS) or two (quantum cutting, QC) NIR photon(s). The NIR emission of Yb has been merged in this field coupled with different ions such as Nd,[9] Er,[10] Tm,[11] and Pr[12].However, the interesting optical features of both Ce and Yb, coupled together, push up the expected level of the quantum efficiency conversion, at optimum conditions, to approx. 200%[13-15]. This is particularly attributable to the unique optical properties of Ce. It has large UV/visible absorption cross-section with tunable emission, depending on the host material, that can be adjusted around 500 nm (20000 cm^{-1}) corresponding to twice the energy required for exciting Yb (less than 10000 cm^{-1})[6-8]. This advantage means that energy transfer from one Ce ion to two Yb ions in its vicinity can be facilitated. Another mechanism for the energy transfer from Ce to Yb has been suggested via charge transfer mediation[16-20]. In such mechanism, Ce^{3+} ions, upon excitation, interact with Yb^{3+} by electron exchange and form a temporary intermediate state from (Ce^{4+} + Yb^{2+}), which relaxes to the $^2F_{5/2}$ excited state of Yb^{3+} and emits NIR photons[8, 21-22]. In contrast to the quantum cutting process, the charge transfer mechanism involves the energy transfer from one Ce ion to one Yb ion. In addition, the probability of back energy transfer from Yb to Ce is expected to be low thanks to the absence of energy sub-levels in Ce. Consequently, Ce ions can absorb significant part of UV-Visible solar radiation then transfer it to Yb ion(s) that subsequently emit at the maximum absorption response of silicon solar cell. Hence, coating solar cell with Ce and Yb-containing transparent layer is a promising approach to increase the cell efficiency. The high UV-Visible optical transparency and the excellent chemical and mechanical properties of AlN make it a good candidate in this direction. It can transmit the solar radiation in the target region and act as a protective layer for the solar cell. However, oxygen is considered as a dominant impurity in AlN host. Hence,

producing AlN free from oxygen is very difficult. In addition, we evidenced in a previous work[23] that 7% of oxygen was required in order to activate the luminescence from Ce in AlN matrix. Therefore, in the present study, for comparison purposes, all Yb doped samples, single and co-doped, have been prepared in Al(O)N hosts with 7% of oxygen. Moreover, we have shown that 7% of oxygen in AlN do not modify the structure and local bonding of the AlN matrix, as evidenced by XRD and EELS measurements. Because, to the best of our knowledge, coupling of Ce and Yb in Al(O)N has never been reported.

This study focuses on elementary optical excitation, transfer and emission mechanisms in Ce, Yb co-doped Al(O)N thin films.

2. Experimental section

Radio frequency (RF) balanced reactive magnetron sputtering is used for preparation of the Al(O)N thin films with single and co-doped by Ce and Yb. Details of the experimental setup can be found in[24]. Specifically, for co-doping, a modified aluminum disk of 2 inch diameter was used that incorporates a thin bar of metallic Ce along with attached metallic piece of Yb allowing to obtain a constant concentration of Ce and different Yb contents. In this approach, the Yb content can be modified by changing the size of the Yb metal piece such that the surface area of Yb metal exposed to the sputtering process is modified. A high vacuum pressure of 1×10^{-6} Pa was reached thanks to a turbo molecular pump (BOC EDWARDS EXT 255HI) coupled to a mechanical primary pump. Constant gas composition of argon and nitrogen (65% nitrogen) was controlled by adjusting the argon and nitrogen gas flow rates and keeping the total pressure (0.7 mtorr) constant using an MKS mass flow controller. A leak of oxygen was applied using *all-metal gas regulating valve* allowing a fine control of the oxygen partial pressure at 10^{-7} torr. This led to Ce, Yb co-doping in the hexagonal wurtzite structure of aluminum oxynitride matrix, Al(O)N, with ~7 at.% of oxygen. The composition was analyzed with a 5MV accelerator at *Centro de Microanálisis de Materiales* (CMAM, Madrid) using Rutherford backscattering spectrometry (RBS) under 2 MeV He^+ beam. Silicon (100) substrates have been used after cleaning in ethanol and then placed at 5 cm distance from the Al target, facing the target axis. X-ray diffraction (XRD) measurement have been performed by using a Brucker D8 Advance system with Cu $K_{\alpha1}$ radiation (λ= 0.15406 nm) in Bragg-Brentano geometry. The microstructure was investigated by transmission electron microscopy (TEM) in a JEOL ARM 200-Cold equipped with a field-emission gun (FEG) fitted with a GIF Quantum ER. The deposition time was adjusted to reach a thickness close to 200 nm. The

samples underwent a *post*-deposition rapid thermal annealing (RTA) at 1000 ^{o}C in forming gas (FG) (N_2/H_2 %=90/10) for 5 minutes. Steady state PL experiments were performed at room temperature. He-Cd laser with 325 nm line has been used to excite the samples. For PLE spectroscopy, a xenon arc lamp was used as excitation source and a cooled silicon-based CCD camera was used for detecting and analyzing the PL emission. For time-resolved photoluminescence measurement, Samples were pumped by 355 nm line of a frequency-tripled YAG:Nd laser with 10 ns, 10 mJ and 10 Hz pulse duration, pulse energy, and repetition rate; respectively. The emitted light was detected by a monochromator equipped with photomultiplier tube and analyzed by GHz Oscilloscope.

3. Results and discussion

Figure 1 shows the RBS spectra that have been measured mainly to probe the Ce and Yb contents in the prepared samples. Each region is labelled based on constitutive elements (Ce, Yb, Al, Si, O, and N). It appears that Ce and Yb signals are partially overlapped. The contributions related to Ce and Yb components in the RBS spectra can be discriminated as shown in inset figure 1. The maximum energy of backscattered projectiles is given by the kinematic factor of the collision and corresponds to scattering events occurring at the surface of each film. The broadness and shape of the film-containing elements is an indication of the film thickness and the elemental profile, respectively. It can be observed that, due to the similar mass of Ce and Yb, the signal from both elements is partially overlapped. Hence, as the content of Yb increases, the overlapped area of the band that corresponds to Ce and Yb increases. Fitting of the spectra revealed no significant changes in the relative elemental composition of the host matrix (~ 46 at.% Al, ~ 45 at.% N, and ~ 7 at.% O) between the five samples. On the other hand, the Ce content was found constant ~1.5 at.% with different contents of Yb% (0,0.6, 0.8, 1, and 1.5 at.%) depending on the deposition conditions.

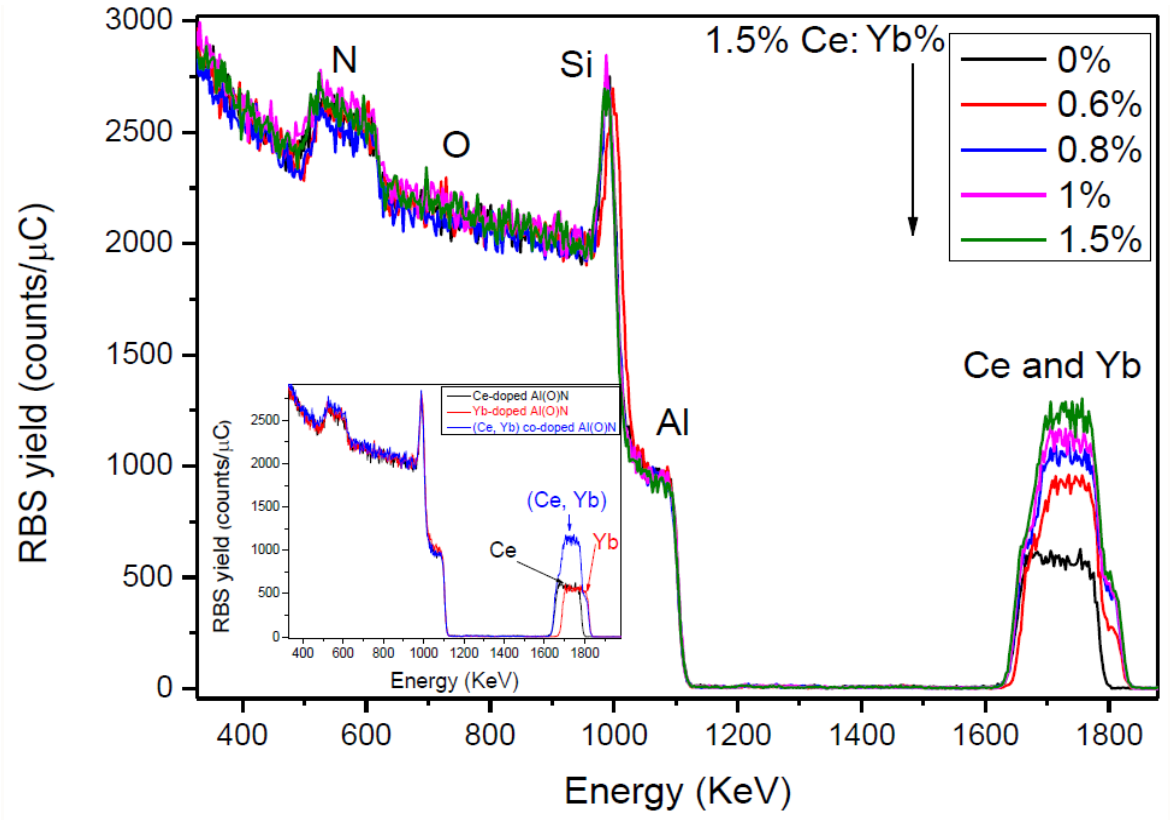

Figure 1. RBS spectra for the prepared (Ce, Yb) co-doped Al(O)N samples at different Yb%. Inset fig. RBS spectra for Ce and Yb singly-doped samples and a co-doped sample with 0.8%Yb.

Figure 2a and b show the X-ray diffractograms of the prepared co-doped samples. Two diffraction peaks corresponding to (002) and (100) planes of AlN can be detected with evolution of the preferential orientation from (002) to (100) as Yb% increases. The zoom in fig (2b) shows the absence of the diffraction peak corresponding to (100) in 0.6%Yb sample, while in 1.5%Yb sample the XRD shows only the signal from (100) AlN. This highlights the influence of the Yb content on the preferential orientation of AlN. Besides showing the highest crystallinity, the sample with 0.8% Yb also exhibits the highest texture coefficient ($T_{(002)}$), calculated using the formula in[24]. $T_{(002)}$ evolves as follows: 0.6 %Yb = 1, 0.8 %Yb = 1.5, 1 %Yb = 0.5, 1.5 %Yb = 0.

The polycrystalline nature of the (1.5% Ce, 0.8% Yb) co-doped Al(O)N sample, has also been evidenced using TEM and selected area electron diffraction (SAED) measurements, figure 2c and d. The microstructure shows a columnar structure with preferential growth direction along the c-axis of the hexagonal wurtzite cell, i.e. along the [002] direction, as shown in figure 2c. The partial rings in the SAED highlight the polycrystalline growth pattern with brightest spots pointing to the predominant growth direction, [002], perpendicular to the substrate.

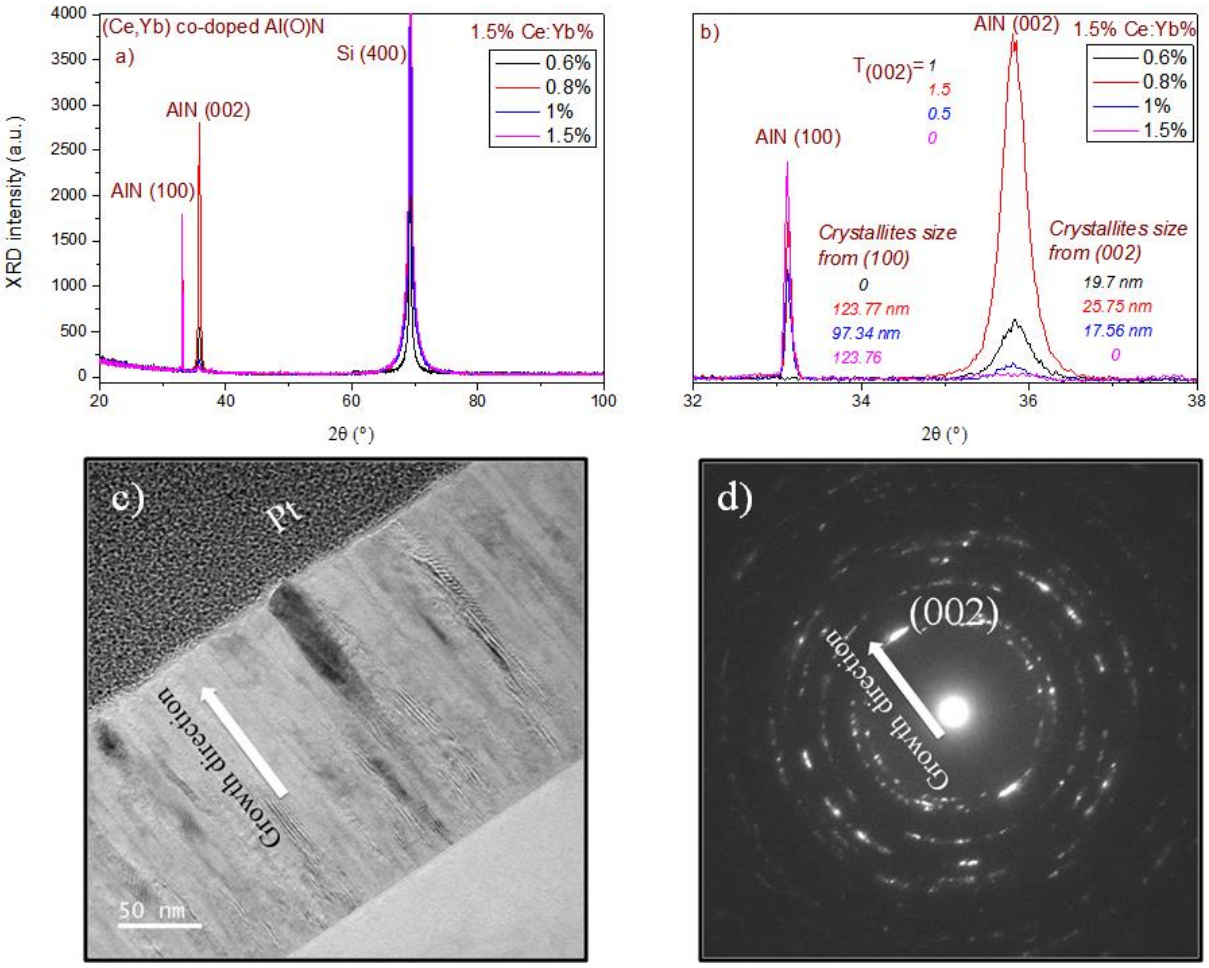

Figure 2. a) X-ray diffractograms of (Ce, Yb) co-doped Al(O)N samples for constant 1.5% Ce and different Yb contents. b) Zoom in of (a) for better visualization indicating values for the average crystallite size and texture coefficient. c) and d) TEM image and SAED pattern of (1.5% Ce, 0.8% Yb) co-doped Al(O)N sample; respectively.

The PL spectra of (Ce, Yb) co-doped Al(O)N for different concentrations of Yb along with single Ce-doped Al(O)N have been measured, figure 3a. The spectra show broad and narrow bands in visible and NIR regions; respectively. The two bands in visible region, around 400 nm and 500 nm, can be ascribed to overlapping between the emissions from Ce ions and host matrix radiative defects. It can hardly be de-convoluted[25-26]. In the NIR region, the single sharp peak around 976 nm is assigned to the optical transition in Yb from $^2F_{5/2}$ to $^2F_{7/2}$. It can also be observed, at the base of Yb emission peak, a small wide band which is referred to the overlapping of unresolved lines, see figure 3b for better visualization.

The PL intensity evolution as a function of the Yb content is shown in the inset figure 3a. Only the Ce emission band is obtained at 0% of Yb. Its intensity decreases upon Yb addition. This is accompanied with increasing intensity of the Yb emission that reaches its maximum

value at 0.8% of Yb. At higher Yb content, it decreases. This can be considered as a sign of energy transfer from Ce and Yb[17, 27-29].

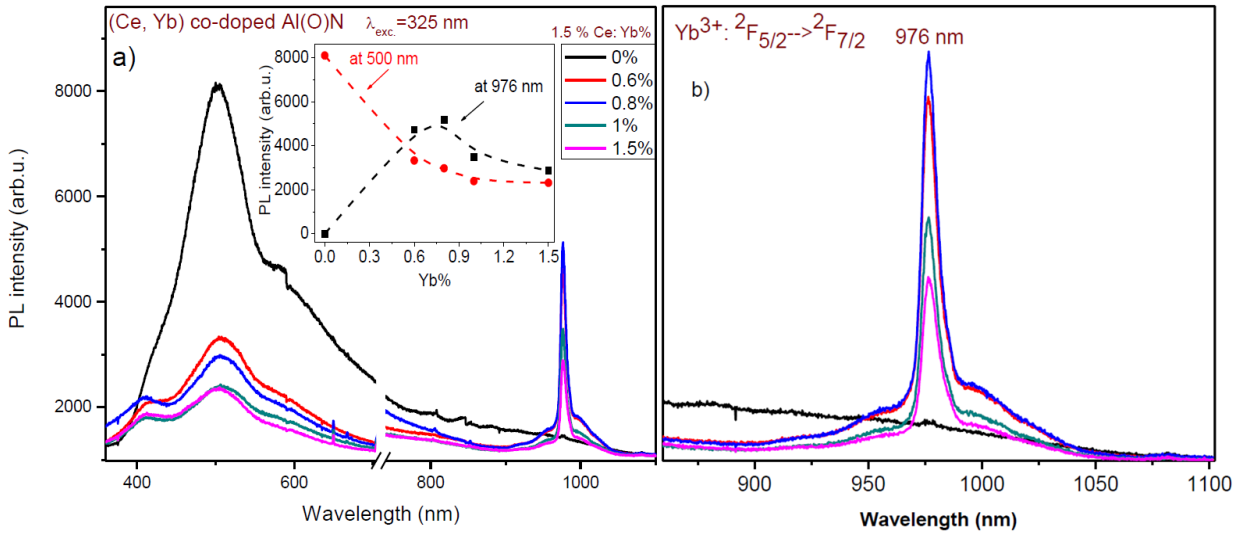

Figure 3. PL spectra of (Ce, Yb) co-doped Al(O)N samples for different Yb concentrations. inset figure: evolution of the PL intensity for the peaks centered at 500 nm and 976 nm as a function of Yb%. b) Zoom in the NIR region.

This decrease in the PL intensity for Yb emission above 0.8%, is attributed to the concentration quenching phenomenon[30]. In this case, a resonant non-radiative energy transfer between excited and un-excited Yb ions can be significant. In addition, a higher density of lattice defects/impurities can be induced by the incorporation of large amount of Yb and act as quenching centers for the PL. It is worth to note that the highest NIR emission intensity is found for 0.8 at.% Yb, in line with the highest crystallinity for this sample among the explored conditions. This could point to the role of crystallinity of the host matrix in enhancing the energy transfer process and/or decreasing the effect of the PL quenching owing to a lower density of lattice defects.

In addition, assuming energy transfer from Ce to Yb essentially infers the contribution of the excitation band(s) of Ce in the excitation spectrum monitored at the Yb PL peak emission 976 nm. Thus, information about the excitation mechanism in the co-doped sample is needed. For this purpose, photoluminescence excitation (PLE) is established as a powerful tool to justify such energy transfer between Ce and Yb[22]. Figure 4 shows the PLE spectra recorded from the (Ce, Yb) co-doped Al(O)N sample containing 0.8% Yb and monitored at emission peaks of 500 nm and 976 nm. For the sake of comparison, the PLE from single Ce-doped Al(O)N sample was also collected at 500 nm. The PLE spectra mainly consist of two bands centered

on 3.9 eV and 4.7-5 eV. Details about the origin of these PLE bands can be found in our previous works and are ascribed to overlapping of Ce and $(V_{Al}\text{-}O_N)^{2-}$ defect complex absorptions (at 3.9 eV) and to $(V_{Al}\text{-}2O_N)^{1-}$ defect complex absorption at 4.8 eV[25, 31]. Interestingly, at 3.9 eV, the PLE spectrum in co-doped sample monitored at the Yb-related PL peak, at 976 nm, shows similar band shape to the PLE bands monitored at Ce related PL peak at 500 nm in the single-doped and co-doped samples.

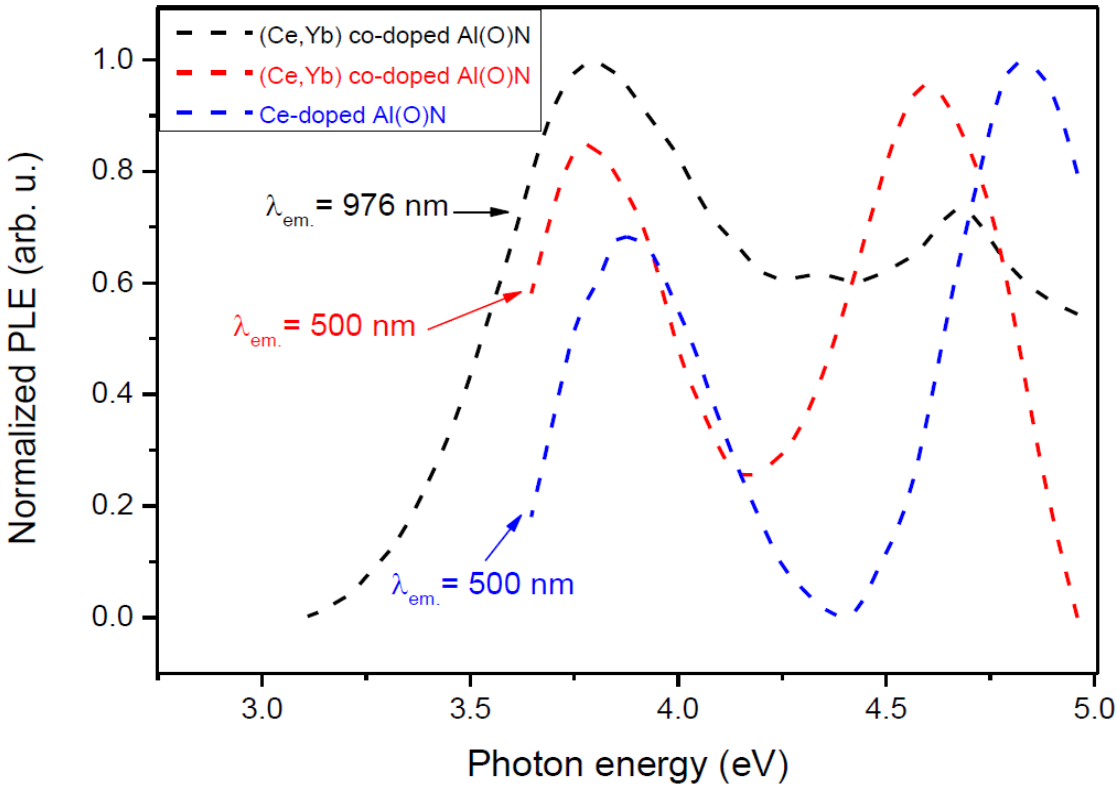

Figure 4. PLE spectra of (1.5 at.% Ce, 0.8 at.% Yb) co-doped Al(O)N sample monitored at 976 nm and 500 nm along with the PLE of 1.5 at.% Ce-doped Al(O)N sample monitored at 500 nm.

This evidences the energy transfer between the two ions[28, 32].Thus, it can be suggested that the absorption of Ce contributes in the NIR emission of Yb^{3+}. Two possible energy transfer mechanisms between Ce and Yb are established: one-*to-two* photons mechanism via cooperative energy transfer and *one-to-one* photon via charge transfer state mechanism. The former is described by the energy transfer from one excited Ce ion to two Yb ions, resulting in emission of two NIR photons. In contrast, the later is described by the energy transfer from one excited Ce ion to one Yb ion, inducing emission of only one NIR photon.

Getting insight into the energy transfer mechanism requires investigation of the PL dynamics between the two ions. Therefore, time resolved photoluminescence (TRPL) measurements

probing the decay time of Yb emission at 976 nm of (Ce, Yb) co-doped Al(O)N sample and comparison with the TRPL collected from single Yb-doped Al(O)N have been performed, see figure 5. The rise and decay times of Yb ions have been monitored in 1 at.% Yb-doped Al(O)N, (1.5 at.% Ce, 0.8 at.% Yb) co-doped Al(O)N and (1.5 at.% Ce, 1at. %Yb) co-doped Al(O)N samples. Despite the (1.5 at.% Ce, 0.8 at.% Yb) co-doped Al(O)N is the optimum sample, the TRPL of (1.5 at.% Ce, 1at. %Yb) co-doped Al(O)N is shown for comparison with the available reference single doped sample, 1 at.% Yb-doped Al(O)N.

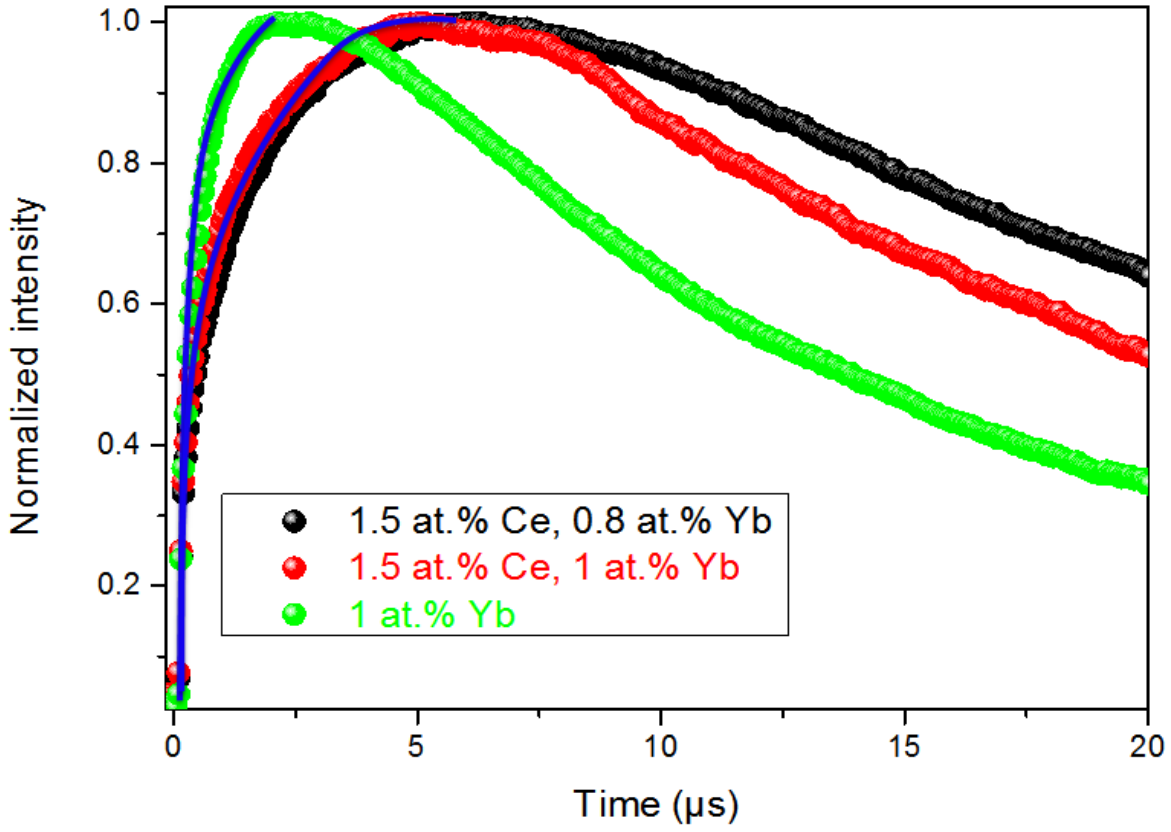

Figure 5.TRPL collected at 976 nm form 1at.%Yb-doped Al(O)N, (1.5 at.% Ce, 0.8 at. %Yb) co-doped Al(O)N and (1.5 at.% Ce, 1at. %Yb) co-doped Al(O)N. The blue bold lines are to guide the readers for the rise time part of the curves.

The average decay lifetime of Yb ions(τ) in single and co-doped samples have been estimated using the following equation:[33-34]

$$\tau = \frac{\int_0^\infty t\, I(t) dt}{\int_0^\infty I(t) dt}, \quad (1)$$

where *I*(t) is the intensity at time t.

This integral formula is used to estimate the average lifetime because of the different decay transitions involved in the energy transfer process. The average lifetime of Yb^{3+} is close to 65μs in single and co-doped cases. This infers undetectable influence of Ce on the decay behavior of Yb^{3+} emission. However**,** the rise time is slower in the co-doped samples, as shown in figure 5. It is found that the rise times of Yb-doped Al(O)N and (Ce, Yb) co-doped Al(O)N are best fitted by single exponential growth function and results in average rise times of τ_1= 0.37 μs and 1.19 μs; respectively. This infers that Yb^{3+} is excited through a slower pathway in the co-doped system. Whereas, in single Yb-doped Al(O)N the excitation mechanism is mediated via defect complex $(V_{Al}\text{-}O_N)^{2-}$[31]. The present results strongly suggests that, in (Ce, Yb) co-doped Al(O)N, the energy transfer mechanism is mediated by Ce ions that stretch the excitation process of Yb^{3+}. In addition, the rise time in co-doped sample is longer than the expected fast decay time, of few nanoseconds, of Ce. This rules out the anticipation of a direct energy transfer process from Ce to Yb. Direct energy transfer from Ce to Yb would be associated to a rise time shorter than the relaxation time of the 5*d* level in Ce^{3+}[17]. The long rise time obtained suggests that the energy transfer for Ce^{3+} to Yb^{3+} is achieved through an indirect process. It is due to slow nonradiative relaxation from a charge transfer state (CTS) to the upper $^2F_{5/2}$ excited state of Yb^{3+}, as suggested by J. Ueda et al[17]. Therefore, different overlapped transitions can be suggested to be involved in the energy transfer process; from Ce to CTS, then CTS to Yb $^2F_{5/2}$ excited state and, finally, from $^2F_{5/2}$ to $^2F_{7/2}$.

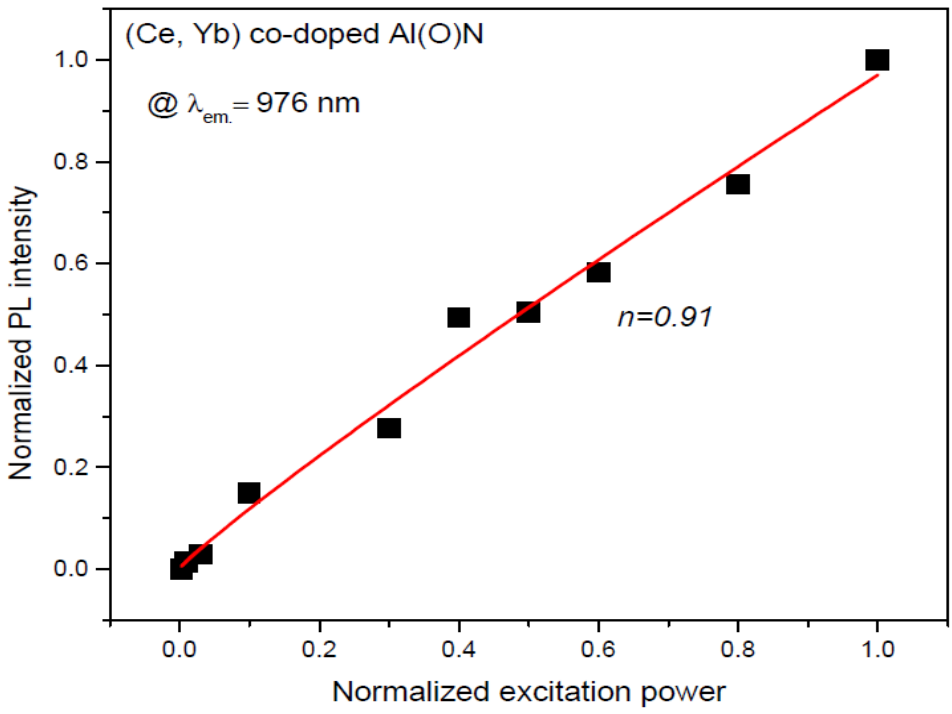

Figure 6. PL power-dependent of Yb emission at 976 nm from (1.5 at.% Ce, 1 at.% Yb) co-doped sample excited by 325 nm.

In this direction, power-dependent PL measurements were performed to study the conversion mechanism from UV/Visible to NIR[35-36]. A power law ($I_{PL} \propto P^n$) is used, where I_{PL} is the PL intensity, P is the excitation power and n is corresponding to the number of transferred photons that produce one NIR photon[35-37]. The power dependent measurement for the (Ce, Yb) co-doped system reveals a nearly linear dependence with n close to 1, as shown in figure 6. This supports our conclusion from lifetime measurements that the energy transfer from Ce to Yb occurs through CTS mechanism, i.e. through a *one-to-one* photon mechanism. This CTS can be attributed to the following electron transfer mechanism: $Ce^{3+} + Yb^{3+} \Rightarrow Ce^{4+} + Yb^{2+}$.

4. Conclusion

(Ce, Yb) co-doped thin films have been prepared with 1.5 at.% Ce and different concentrations of Yb (0.6%, 0.8%, 1%, 1.5%). RBS spectrometry was used to determine the elemental contents of the prepared samples. XRD and TEM measurements revealed the polycrystalline nature of all samples and strong (002) preferential orientation and high crystallinity of (1.5% Ce, 0.8% Yb) sample. In addition, this sample showed maximum NIR emission intensity, which points to presence of optimum Ce and Yb contents for maximum energy transfer from UV to NIR. Hence, The energy transfer between Ce and Yb was achieved and evidenced through: i) The evolution of the PL intensity as a function of Yb%, ii) Participation of the excitation band of Ce in the PLE for emission of Yb^{3+}, and iii) Stretching of the excitation rise time of Yb^{3+} in co-doped system compared to the single Yb-doped system. In addition, the energy transfer is found to proceed by *one-to-one* photon mechanism mediated through CTS as proposed from the excitation rise time behavior and confirmed by PL power-dependent measurement.

Acknowledgments

A.E. Giba thanks the financial support from Erasmus mundus scholarship within the DocMASE program. He also thanks the ”Université franco-allemande” (UFA) for supporting his travel and stay to Saarland University within the PhD-track program. Financial support from grant P2013/MIT-2775 (Comunidad Autónoma de Madrid, Spain) is greatly

acknowledged. EIT raw Materials SPARK project is acknowledged for support with travel expenses.

References

[1] Huang X Y, Yu D C and Zhang Q Y 2009 *J. Appl. Phys.* **106** 113521
[2] Zhou W, Yang J, Wang J, Li Y, Kuang X, Tang J and Liang H 2012 *Opt. Express* **20** A510-A8
[3] Zhang Q, Wang J, Zhang G and Su Q 2009 *J. Mater. Chem.* **19** 7088-92
[4] Liu T-C, Zhang G, Qiao X, Wang J, Seo H J, Tsai D-P and Liu R-S 2013 *Inorg. Chem.* **52** 7352-7
[5] Zhou D, Liu D, Pan G, Chen X, Li D, Xu W, Bai X and Song H 2017 *Adv. Mater.* **29** 1704149
[6] Meijer J-M, Aarts L, van der Ende B M, Vlugt T J H and Meijerink A 2010 *Phys.Rev.B* **81** 035107
[7] Florêncio L d A, Gómez-Malagón L A, Lima B C, Gomes A S L, Garcia J A M and Kassab L R P 2016 *Sol. Energy Mater Sol. Cells* **157** 468-75
[8] Li J, Chen L, Hao Z, Zhang X, Zhang L, Luo Y and Zhang J 2015 *Inorg. Chem.* **54** 4806-10
[9] Chen D, Yu Y, Lin H, Huang P, Shan Z and Wang Y 2010 *Opt. Lett.* **35** 220-2
[10] Aarts L, Jaeqx S, van der Ende B M and Meijerink A 2011 *J. Lumin.* **131** 608-13
[11] Lin H, Zhou S, Hou X, Li W, Li Y, Teng H and Jia T 2010 *IEEE Photonic Tech. Lett.* **22** 866-8
[12] Xu Y, Zhang X, Dai S, Fan B, Ma H, Adam J-l, Ren J and Chen G 2011 *J. Phys. Chem. C* **115** 13056-62
[13] Gao B, Yan Q, Tong Y, Zhang X, Ma H, Adam J-l, Ren J and Chen G 2013 *J. Lumin.* **143** 181-4
[14] Zhang H, Chen J and Guo H 2011 *J. Rare Earth.* **29** 822-5
[15] Tai Y, Li X, Du X, Pan B and Yuan G 2018 *RSC Adv.* **8** 23268-73
[16] You F, Bos A J J, Shi Q, Huang S and Dorenbos P 2011 *J. Phys. Condens. Matter.* **23** 215502
[17] Ueda J and Tanabe S 2009 *J. Appl. Phys.* **106** 043101
[18] Verweij J W M, Pédrini C, Bouttet D, Dujardin C, Lautesse H and Moine B 1995 *Opt. Mater.* **4** 575-82
[19] Cooke D W, Muenchausen R E, Bennett B L, McClellan K J and Portis A M 1998 *J. Lumin.* **79** 185-90
[20] Rivas-Silva J F, Durand-Niconoff S, Schmidt T M and Berrondo M 2000 *Int. J. Quantum Chem.* **79** 198-203
[21] Heng C L, Wang T, Su W Y, Wu H C, Yin P G and Finstad T G 2016 *J. Appl. Phys.* **119** 123105
[22] Yu D C, Rabouw F T, Boon W Q, Kieboom T, Ye S, Zhang Q Y and Meijerink A 2014 *Phys. Rev. B* **90** 165126
[23] Giba A E, Pigeat P, Bruyere S, Rinnert H, Soldera F, Mücklich F and Horwat D 2018 *J. Phys. Chem. C* **122** 21623-31
[24] Giba A E, Pigeat P, Bruyère S, Easwarakhanthan T, Mücklich F and Horwat D 2017 *Thin Solid Films* **636** 537-45

[25] Giba A E, Pigeat P, Bruyere S, Rinnert H, Soldera F, Mücklich F, Gago R and Horwat D 2017 *ACS Photonics* **4** 1945-53
[26] Cao Y G, Chen X L, Lan Y C, Li J Y, Xu Y P, Xu T, Liu Q L and Liang J K 2000 *J. Cryst. Growth* **213** 198-202
[27] Liu X, Teng Y, Zhuang Y, Xie J, Qiao Y, Dong G, Chen D and Qiu J 2009 *Opt. Lett.* **34** 3565-7
[28] Liu Z, Li J, Yang L, Chen Q, Chu Y and Dai N 2014 *Sol. Energy Mater Sol. Cells* **122** 46-50
[29] Chen D, Wang Y, Yu Y, Huang P and Weng F 2008 *J. Appl. Phys.* **104** 116105
[30] Lin H, Zhou S, Teng H, Li Y, Li W, Hou X and Jia T 2010 *J. Appl. Phys.* **107** 043107
[31] 2018 *J. Appl. Phys.* **124** 033102
[32] Kumar K S, Lou C, Manohari A G, Huihui C and Pribat D 2017 *RSC Adv.* **7** 24674-8
[33] Li L, Lou C, Sun X, Xie Y, Hu L and Kumar K S 2016 *ECS J. Solid State Sci. Technol.* **5** R146-R9
[34] Jia Y, Qiao H, Zheng Y, Guo N and You H 2012 *PCCP* **14** 3537-42
[35] Strek W, Deren P and Bednarkiewicz A 2000 *J. Lumin.* **87** 999-1001
[36] Stręk W, Bednarkiewicz A and Dereń P J 2001 *J. Lumin.* **92** 229-35
[37] Terra I A A, Borrero-González L J, Figueredo T R, Almeida J M P, Hernandes A C, Nunes L A O and Malta O L 2012 *J. Lumin.* **132** 1678-82

Figures captions

Figure 1. RBS spectra for the prepared (Ce, Yb) co-doped Al(O)N samples at different Yb%. Inset fig. RBS spectra for Ce and Yb singly-doped samples and a co-doped sample with 0.8%Yb.

Figure 2. a) X-ray diffractograms of (Ce, Yb) co-doped Al(O)N samples for constant 1.5% Ce and different Yb contents. b) Zoom in of (a) for better visualization indicating values for the average crystallite size and texture coefficient. c) and d) TEM image and SAED pattern of (1.5% Ce, 0.8% Yb) co-doped Al(O)N sample; respectively.

Figure 3. PL spectra of (Ce, Yb) co-doped Al(O)N samples for different Yb concentrations. inset figure: evolution of the PL intensity for the peaks centered at 500 nm and 976 nm as a function of Yb%. b) Zoom in the NIR region.

Figure 4. PLE spectra of (1.5 at.% Ce, 0.8 at.% Yb) co-doped Al(O)N sample monitored at 976 nm and 500 nm along with the PLE of 1.5 at.% Ce-doped Al(O)N sample monitored at 500 nm.

Figure 5.TRPL collected at 976 nm form 1at.%Yb-doped Al(O)N, (1.5 at.% Ce, 0.8 at. %Yb) co-doped Al(O)N and (1.5 at.% Ce, 1at. %Yb) co-doped Al(O)N. The blue bold lines are to guide the readers for the rise time part of the curves.

Figure 6. PL power-dependent of Yb emission at 976 nm from (1.5 at.% Ce, 1 at.% Yb) co-doped sample excited by 325 nm.